AJNR

Arterial Spin-Labeling Perfusion Metrics in Pediatric Posterior Fossa Tumor Surgery

S.M. Toescu, P.W. Hales, J. Cooper, E.W. Dyson, K. Mankad, J.D. Clayden, K. Aquilina and C.A. Clark

AJNR Am J Neuroradiol 2022, 43 (10) 1508-1515
doi: https://doi.org/10.3174/ajnr.A7637
http://www.ajnr.org/content/43/10/1508

Arterial Spin-Labeling Perfusion Metrics in Pediatric Posterior Fossa Tumor Surgery

S.M. Toescu, P.W. Hales, J. Cooper, E.W. Dyson, K. Mankad, J.D. Clayden, K. Aquilina, and C.A. Clark

ABSTRACT

BACKGROUND AND PURPOSE: Pediatric posterior fossa tumors often present with hydrocephalus; postoperatively, up to 25% of patients develop cerebellar mutism syndrome. Arterial spin-labeling is a noninvasive means of quantifying CBF and bolus arrival time. The aim of this study was to investigate how changes in perfusion metrics in children with posterior fossa tumors are modulated by cerebellar mutism syndrome and hydrocephalus requiring pre-resection CSF diversion.

MATERIALS AND METHODS: Forty-four patients were prospectively scanned at 3 time points (preoperatively, postoperatively, and at 3-month follow-up) with single- and multi-inflow time arterial spin-labeling sequences. Regional analyses of CBF and bolus arrival time were conducted using coregistered anatomic parcellations. ANOVA and multivariable, linear mixed-effects modeling analysis approaches were used. The study was registered at clinicaltrials.gov (NCT03471026).

RESULTS: CBF increased after tumor resection and at follow-up scanning ($P = .045$). Bolus arrival time decreased after tumor resection and at follow-up scanning ($P = .018$). Bolus arrival time was prolonged ($P = .058$) following the midline approach, compared with cerebellar hemispheric surgical approaches to posterior fossa tumors. Multivariable linear mixed-effects modeling showed that regional perfusion changes were more pronounced in the 6 children who presented with symptomatic obstructive hydrocephalus requiring pre-resection CSF diversion, with hydrocephalus lowering the baseline mean CBF by 20.5 (standard error, 6.27) mL/100g/min. Children diagnosed with cerebellar mutism syndrome (8/44, 18.2%) had significantly higher CBF at follow-up imaging than those who were not ($P = .040$), but no differences in pre- or postoperative perfusion parameters were seen.

CONCLUSIONS: Multi-inflow time arterial spin-labeling shows promise as a noninvasive tool to evaluate cerebral perfusion in the setting of pediatric obstructive hydrocephalus and demonstrates increased CBF following resolution of cerebellar mutism syndrome.

ABBREVIATIONS: AIC = Akaike information criterion; ASL = arterial spin-labeling; BAT = bolus arrival time; BuxCBF = Buxton-modeled CBF from multi-TI ASL data; CMS = cerebellar mutism syndrome; EVD = external ventricular drain; HCP = hydrocephalus; ICP = intracranial pressure; mod = model; (mod_hcp) = addition of HCP with an interaction term for the time point; (mod_hcpcms) = full model including terms for CMS and HCP; PLD = post-labeling delay; TI = inflow time

CBF is a physiologic parameter with a well-established relationship to intracranial pressure (ICP) and systemic arterial blood pressure.[1-3] Changes in CBF follow open craniotomy in adult patients,[4] but less is known about the effect of neurosurgery on CBF in children.[5] Brain tumors commonly occur in the posterior fossa in children, who often present with symptoms of raised ICP due to obstruction of CSF flow.[6] Obstructive hydrocephalus (HCP) can be severe enough to warrant emergency CSF diversion as a life-saving procedure before tumor resection. There are few reports of alterations in perfusion metrics in children with HCP.[5,7,8] Following tumor resection, up to one-quarter of patients develop cerebellar mutism syndrome (CMS),[9] characterized by a delayed onset of mutism and emotional lability,[10] which tend to resolve during weeks to months. Damage to the superior cerebellar peduncles is thought to disturb reciprocal cerebrocerebellar pathways, giving rise to the striking symptomatology of the condition. Frontal perfusion deficits in patients with CMS have previously been shown using SPECT imaging,[11,12] DSC MR imaging,[13] and, more recently, arterial spin-labeling (ASL).[14,15]

ASL quantifies brain perfusion in physiologically relevant units by subtracting an image with radiofrequency-labeled blood

Received January 3, 2022; accepted after revision July 27.

From the Departments of Neurosurgery (S.M.T., E.W.D., K.A.) and Neuroradiology (J.C., K.M., C.A.C.), Great Ormond Street Hospital, London, UK; and Developmental Imaging and Biophysics Section (S.M.T., P.W.H., J.D.C.), University College London Great Ormond Street Institute of Child Health, London, UK.

This work was supported by Children With Cancer UK, CwC-UK-15-203, and the Great Ormond Street Hospital Charity, 174385.

Please address correspondence to Sebastian M. Toescu, MD, Developmental Imaging and Biophysics Section, UCL-GOS Institute of Child Health, 30 Guilford St, London, UK, WC1N 1EH; e-mail: Sebastian.toescu@ucl.ac.uk; @sebmigueltoescu

http://dx.doi.org/10.3174/ajnr.A7637

from a control image at a suitable post-labeling delay (PLD, also known as single inflow time [TI] or single-TI data). By acquiring data at multiple TIs (multi-TI), it is possible to extract further parameters such as the bolus arrival time (BAT) of labeled blood. BAT varies regionally, making single-PLD acquisitions susceptible to underestimation of CBF due to incomplete delivery of the bolus of labeled blood at the chosen TI. The advantage of multi-TI ASL is that this issue is accounted for by imaging at serially increasing TIs.

The aim of this study was to characterize perfusion metrics of CBF and BAT of labeled blood using single- and multi-TI ASL in children with posterior fossa tumors. We also aimed to investigate how changes in perfusion metrics were modulated by perioperative surgical and clinical features of CMS and HCP requiring pre-resection CSF diversion. We hypothesized that children with CMS would have reduced CBF postoperatively and that HCP would cause a reduction in preoperative CBF and prolong preoperative BAT.

MATERIALS AND METHODS

Patients

Children referred to our institution with posterior fossa tumors underwent MR imaging before tumor resection, within 72 hours of tumor resection, and at 3-month follow-up. Scans were performed with the patient under general anesthesia in younger children to avoid movement artifacts; otherwise, all scanning was performed in unsedated patients. Sedation requirements were assessed by experienced pediatric neuroradiographers before scanning and were primarily determined by patient age. Only 1 patient required general anesthesia at a follow-up scan appointment, having previously tolerated unsedated scanning.

Children presenting with symptomatic HCP (signs of raised ICP, such as headache, vomiting, or deteriorating conscious levels) were treated with urgent CSF diversion in the form of an external ventricular drain (EVD) before tumor resection. Those who did not undergo pre-resection EVD were temporized with glucocorticoid administration until tumor resection. Operative notes were contemporaneously reviewed, and the intradural surgical approach to the tumor was categorized into midline, hemispheric, and miscellaneous groups. Postoperative CMS status was determined by prospective clinical evaluation by attending neurosurgical and multidisciplinary staff. The diagnosis was primarily based on the presence of mutism or reduced speech output in the early postoperative phase. Patients were followed up at 2 months postoperatively to assess ongoing symptoms of CMS. Ethics approval was granted by the National Health Service Health Research Authority (18/LO/0501), and the study was registered at clinicaltrials.gov (NCT03471026).

MR Imaging Acquisition

Imaging was performed on a 3T MR imaging scanner (Magnetom Prisma; Siemens) using a 20-channel receive head coil. The scanning protocol comprised structural imaging (including T1 MPRAGE), multishell diffusion imaging, and ASL. Imaging at the preoperative time point was acquired before CSF diversion.

Single-PLD ASL was performed using a prototype pseudocontinuous labeling sequence with background suppression and a 3D gradient-echo and spin-echo readout. Imaging parameters were set according to international consensus recommendations,[16] with a labeling duration of 1800 ms, a 1500-ms PLD, and 10 repetitions. The FOV was 220 mm with a 64 × 62 matrix reconstructed to 1.7 × 1.7 mm^2 in-plane spatial resolution (interpolation factor = 2). Additional sequence parameters were the following: 24 partitions; turbo factor = 12; EPI factor = 31; segments = 2 (with parallel imaging, generalized autocalibrating partially parallel acquisition = 2); section thickness = 4.0 mm; TR = 4620 ms; TE = 21.8 ms. A proton density–weighted (M0) image was also acquired, with a readout identical to that of the ASL acquisition but with the labeling radiofrequency pulses removed for CBF quantification.

Multi-TI pulsed ASL data comprised acquisitions at 10 TIs ranging from 350 to 2600 ms in 250-ms steps, with a single acquisition per TI. The TR was 3300 ms; all other readout parameters were the same as above.

Image Processing

Cortical parcellation and subcortical segmentation were performed on volumetric T1-weighted images using FreesSurfer (http://surfer.nmr.mgh.harvard.edu),[17] and these were registered into the patient's diffusion space using Niftyreg (http://sourceforge.net/projects/niftyreg/).[18] Repetitions of raw ASL images were checked for motion artifacts before averaging. Preprocessing of all ASL data was performed in Matlab (R2017b, MathWorks). Single-PLD data were preprocessed using the method of Alsop et al[16] to calculate voxelwise CBF (milliliter/100 g/min). The kinetic model described by Buxton et al[19] was used on noise-masked multi-TI ASL data to calculate voxelwise maps of BAT (seconds) and CBF (milliliter/100g/min; referred to in the Results section as Buxton-modeled CBF from multi-T1 ASL data [BuxCBF] to avoid confusion with CBF from single-PLD data). Details of the model-fitting procedure are described elsewhere.[20] Each patient's ASL parameter maps were registered into the patient's diffusion space using FLIRT[21] (https://fsl.fmrib.ox.ac.uk/fsl/fslwiki/FLIRT). Diffusion space was chosen as a symmetric registration space because its resolution was midway between that of ASL and structural images. Time point– and subject-specific median perfusion parameters were then extracted for regions corresponding to frontal, parietal, occipital, temporal, and motor (precentral, paracentral, and caudal middle frontal gyri) cortices, thalamus, and cerebellum.

Statistical Analysis

Statistical analysis was performed in R (Version 3.6.1).[22] Continuous data were tested for differences in means using a 2-tailed Student *t* test after assessing assumptions of normality using the Shapiro-Wilk test. Non-normally distributed data were tested using the Wilcoxon rank-sum test. A prespecified α of .05 was chosen. A 1-way repeated-measures ANOVA was performed to examine the effect of the scanning time point on perfusion metrics. Subsequent group comparisons using pair-wise *t* tests were corrected for multiple comparisons using the false discovery rate.

A multivariable linear mixed-effects modeling analysis was performed in which subject identification was taken as a random effect, and fixed effects included scanning time point, brain region, age, sedation status, HCP, and CMS. The Akaike information criterion (AIC) and marginal/conditional R^2 values[23] were

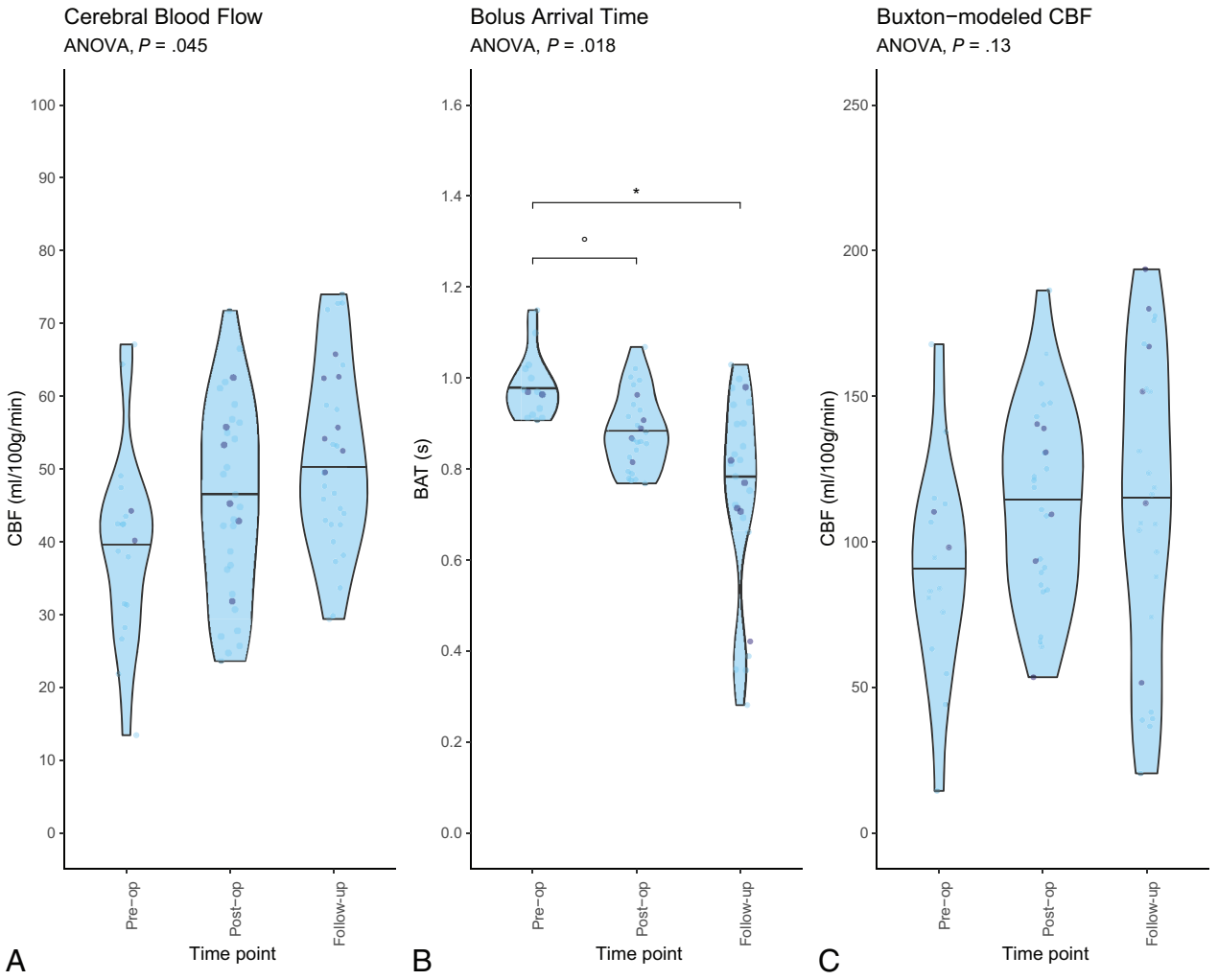

FIG 1. Violin plots showing changes in perfusion metrics across time points for all patients' brain regions. The *horizontal line* within the plot indicates the median. *Darker data points* indicate patients with CMS. *A*, CBF derived from single-PLD ASL. *B*, BAT derived from multi-TI ASL. *C*, CBF derived from multi-TI ASL. *Horizontal significance bars* show false discovery rate–adjusted *P* values from *t* test pair-wise comparisons (*degree sign* indicates $P < .1$; *asterisk*, $P < .05$). Pre-op indicates preoperative; Post-op, postoperative.

used to assess model performance. Model performance was taken to be improved with a lower AIC and/or an increase in R^2. The likelihood ratio ANOVA tests were used to assess the effects of additive model terms.

RESULTS

Forty-four patients were prospectively recruited to the study, with a mean age of 6.69 (SD, 3.68) years; range, 1.04–14.6 years; 23 were female. The most common tumor histology encountered at the operation was pilocytic astrocytoma ($n = 22$), followed by medulloblastoma ($n = 14$), ependymoma ($n = 2$), diffuse midline glioma ($n = 2$), and atypical teratoid/rhabdoid tumor, ganglioglioma, hemangioblastoma, and high-grade glioma (1 each). Six patients (13.6%) underwent preoperative CSF diversion due to symptomatic obstructive HCP. Most patients (23/44, 52.3%) underwent midline intradural surgical approaches to the tumor. Eleven patients (25.0%) underwent lateral transcerebellar hemispheric approaches, and the remaining 10 patients (22.7%) had heterogeneous surgical approaches to their tumor, including biopsy only and cerebellopontine angle or direct access to large tumors presenting to the parenchymal surface. Eight patients (18.2%) were diagnosed with CMS in the postoperative period. The cardinal symptom of mutism was improved in 5 of these patients at follow-up. Eleven patients in the cohort (25.0%, all having medulloblastomas) underwent adjuvant photon radiation therapy.

Change in Gross Perfusion Metrics

Mean CBF in the cerebral cortex increased across the 3 time points (preoperative: 39.6 [SD, 13.3] mL/100g/min; postoperative: 45.5 [SD, 13.3] mL/100g/min; follow-up: 51.5 [SD, 12.6] mL/100g/min; Fig 1*A*). Repeated-measures ANOVA revealed statistically significant differences among the 3 time points ($P = .045$), though post hoc tests did not survive multiple comparison correction. Mean regional BAT decreased with time (preoperative: 0.982 [SD, 0.069] seconds; postoperative: 0.884 [SD, 0.083] seconds; and follow-up: 0.747 [SD, 0.217] seconds; Fig 1*B*). Repeated-measures ANOVA revealed statistically significant differences

among the 3 time points ($P = .018$), and post hoc tests confirmed a significant difference between the preoperative and follow-up time points ($P = .034$). Single-PLD CBF results were echoed by similar trends in mean BuxCBF, though these did not reach statistical significance (preoperative: 90.2 [SD, 36.9] mL/100g/min; postoperative: 113 [SD, 33.3] mL/100g/min; follow-up: 112 [SD, 51.7] mL/100g/min; $P = .129$; Fig 1C). Examples of single-PLD and multi-TI ASL data from a single representative patient are shown in Fig 2.

Table 1 shows differences in perfusion metrics of the cerebral cortex at the postoperative time point, depending on the surgical approach used. There was no significant difference in postoperative CBF between midline and lateral surgical approaches ($P = .212$ and .209, respectively) and no difference in mean age between the 2 groups ($P = .527$). The cortical BAT appeared to be prolonged in children who had undergone a midline approach to the tumor, though this did not reach statistical significance ($P = .058$).

Perfusion and HCP

There was no significant difference in age between those with and without symptomatic obstructive HCP requiring pre-resection CSF diversion ($P = .277$). In patients with HCP, preoperative mean cortical CBF was lower than in those who had not required CSF diversion (mean, 22.2 [SD, 8.95] versus 43.1 [SD, 11.2] mL/100g/min, $P = .032$). These effects were observed for all brain regions studied (Fig 3A), and differences in all regions reached a level of statistical significance apart from the frontal and motor cortices. Postoperatively, mean cortical CBF returned to normal levels, with no statistically significant difference in mean cortical CBF between those who underwent CSF diversion and those who did not (48.3 [SD, 10.7] versus 45.0 [SD, 13.8] mL/100g/min, $P = .562$). At follow-up imaging, mean cortical CBF was 57.5 (SD, 16.5) mL/100g/min in the HCP group compared with 50.3 (SD, 11.8) mL/100g/min in those without HCP ($P = .396$). These results were echoed by the findings from cortical BuxCBF, though they did not reach statistical significance at any time point (all, $P = .183$). Furthermore, a regional analysis did not reveal any statistically significant differences in BuxCBF among groups, other than in the thalamus at the preoperative time point ($P = .014$).

There was a statistically significant prolongation of mean BAT to the cerebral cortex preoperatively in children with symptomatic HCP (1.09 [SD, 0.07] versus 0.954 [SD, 0.037] seconds, $P = .048$). Figure 3B shows that this was more striking in some supratentorial cortical regions, especially the frontal, motor, and occipital. Postoperatively and at follow-up, there were no significant differences in mean cortical BAT depending on pre-resection HCP treatment ($P = .153$ and .558, respectively).

Perfusion and CMS

There was a significant difference in age between children diagnosed with CMS postoperatively and those without (mean, 4.00 [SD,1.90] versus 7.20 [SD, 3.72] years, $P = .002$). Preoperative (42.2 [SD, 2.88] versus 39.3 [SD, 14.1] mL/100g/min, $P = .488$) and postoperative (48.6 [SD, 10.9] versus 44.8 [SD, 13.9] mL/100g/min, $P = .484$) mean cortical CBF was similar between children with CMS and those without. There was a significantly higher mean CBF at the follow-up time point in the CMS group (57.5 [SD, 6.08] versus 49.7 [SD, 13.6] mL/100g/min, $P = .040$). There were no significant differences in BAT or BuxCBF at any time point, and no significant differences in any perfusion metrics on a regional analysis.

Linear Mixed-Effects Modeling

Multivariable linear mixed-effects models were used to explore the effect of HCP and CMS on CBF in the cohort. Models were fit on a 3-region sample of CBF values: the mean across the whole cortex, thalamus, and cerebellum. This

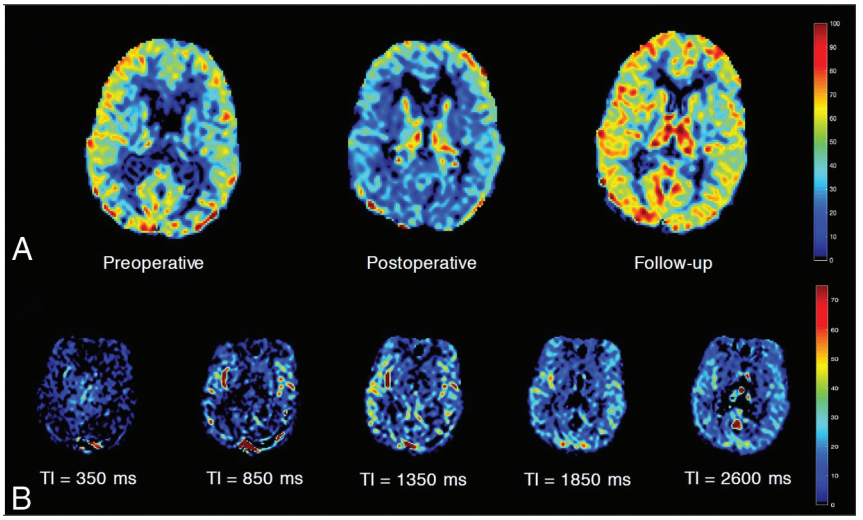

FIG 2. Sample ASL maps of a patient with a posterior fossa pilocytic astrocytoma on a midthalamic axial section. *A*, Single-PLD CBF maps at preoperative, postoperative, and follow-up time points. *Color bar* indicates milliliters/100g/min. *B*, Raw multi-TI ASL data show a difference in magnetization (d*M*) between control and label scans at selected sequentially increasing TIs at a follow-up scan. *Color bar* indicates arbitrary units of *dM*.

Table 1: Mean postoperative cortical perfusion metrics by surgical approach[a]

	Midline	Hemispheric	95% CI Difference	*P*
Age (yr)	6.22 (SD, 3.45)	7.05 (SD, 3.5)	–3.49–1.84	.527
CBF (mL/100g/min)	44.7 (SD, 11.5)	53.4 (SD, 15.5)	–23.3–5.97	.212
BAT (sec)	0.891 (SD, 0.076)	0.828 (SD, 0.056)	–0.002–0.128	.0576
BuxCBF (mL/100g/min)	109 (SD, 27.8)	135 (SD, 42.3)	–70.3–18.6	.209

[a] Values are means and 95% CIs; *P* values are from unpaired *t* tests.

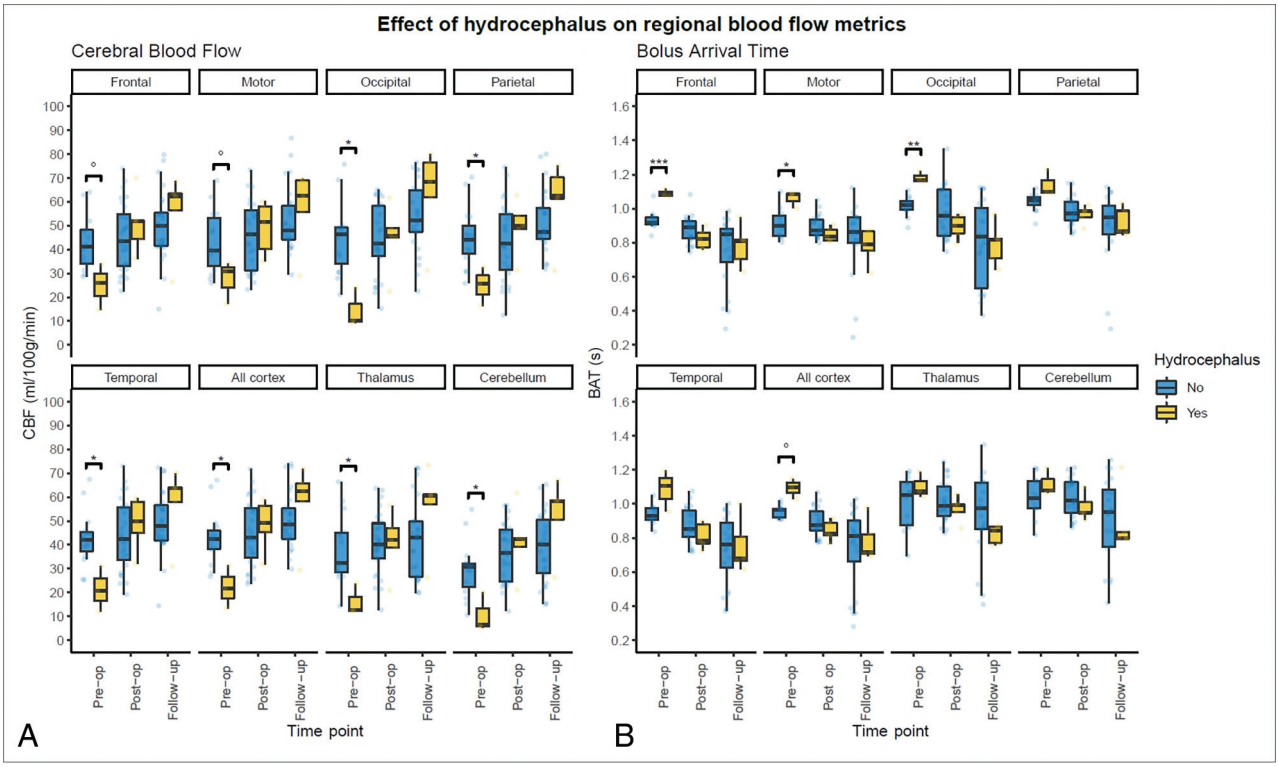

FIG 3. *Boxplots* depicting perfusion metrics stratified by brain regions in patients with and without symptomatic HCP. *A*, CBF derived from single-PLD ASL. *B*, BAT derived from multi-TI ASL. False discovery rate–adjusted *P* values: Degree sign indicates $P < .1$; *asterisk*, $P < .05$; *double asterisks*, $P < .01$; *triple asterisks*, $P < .001$. Pre-op indicates preoperative; Post-op, postoperative.

process began with the fitting of a baseline model (mod_baseline), which did not include the effects of interest, to estimate the effects of time point, age, and brain region on CBF. Model terms and their fixed-effect coefficients are shown in Table 2, along with comparisons of model characteristics.

The addition of HCP with an interaction term for time point (mod_hcp) reduced the AIC and increased R^2 values. Likelihood ratio testing of (mod_hcp2) and (mod_baseline) indicated a significant effect of HCP and its interaction with the time point on the model ($P < .001$). The full model (mod_hcpcms) included terms for CMS and HCP and their interactions with the time point. Likelihood ratio testing between the 2 best-performing models, (mod_hcp) and (mod_hcpcms), showed a statistically significant difference between the 2 in favor of the full model ($P = .03$), which also had the lowest AIC and higher R^2 values.

DISCUSSION

In this prospective study of children with posterior fossa tumors, mean cortical CBF increased after tumor resection and at follow-up imaging. For the first time, we show reductions in the BAT of labeled blood to the cerebral cortex after tumor resection. Children presenting with symptomatic obstructive HCP requiring pre-resection CSF diversion had significantly reduced preoperative CBF and prolonged BAT. A regional analysis according to standardized brain parcellations revealed that CBF was significantly lower preoperatively in many cortical regions in patients with HCP and that BAT was significantly prolonged in the frontal, motor, and occipital cortices of patients with HCP. There was a significantly higher CBF at follow-up in children who developed CMS. A multivariable linear mixed-effects modeling approach confirmed that both HCP and CMS had a powerful effect on CBF by time point. In fact, these 2 factors emerged as more significant features of determining postoperative CBF in the final model than the time point alone.

Our results indicate weak evidence of prolonged BAT after midline approaches to posterior fossa tumors, which entail more extensive dissection of neural parenchyma, greater exposure of CSF spaces, and increased handling and manipulation of large infratentorial arteries, such as the PICA. It is possible that vasospasm could have led to prolonged BAT following midline approaches. This scenario has been described following posterior fossa tumor resection in children[24,25] and even described as a cause of CMS in an adolescent.[26]

Perfusion Metrics and Hydrocephalus

Seventy-to-ninety percent of children with posterior fossa tumors present with HCP.[27] However, the relation between ventricular size, compliance, and pressure is complex, and ventricular size can be equivocal with regard to underlying CSF mechanics.[28] In this series, the need for pre-resection CSF diversion was judged clinically by experienced pediatric neurosurgeons on the basis of features of raised ICP. It is to be expected that resection of a posterior fossa tumor alone will increase CBF due to the removal of an obstructing mass;[5] however, we demonstrate that in patients with symptomatic HCP before tumor resection, the mean cortical CBF was lower and BAT was higher, with statistically significant differences in these parameters among groups.

Table 2: Multivariable linear mixed-effects modeling of CBF based on clinical, demographic, and study factors[a]

	Mod_Baseline	Mod_HCP	Mod_HCPCMS
(Intercept)	43.3 (3.86)[b]	48.4 (4.06)[b]	50.1 (4.70)[b]
Postop time point	6.21 (2.00)[c]	3.01 (2.08)	1.55 (2.20)
Follow-up time point	14.8 (2.07)[b]	10.5 (2.15)[b]	7.74 (2.31)[b]
Age	−0.686 (0.45)	−1.17 (0.53)[d]	−1.34 (0.59)[d]
Thalamus	−5.55 (1.60)[b]	−5.59 (1.51)[b]	−5.60 (1.45)[b]
Cerebellum	−10.0 (1.59)[b]	−10.0 (1.50)[b]	−10.0 (1.44)[b]
Unsedated (vs GA)	–	3.57 (3.79)	5.73 (3.93)
Hydrocephalus	–	−19.4 (6.04)[c]	−20.5 (6.27)[c]
Postop time point + HCP	–	21.5 (5.17)[b]	24.0 (5.13)[b]
Follow-up time point + HCP	–	26.0 (5.22)[b]	27.2 (5.18)[b]
CMS	–	–	−10.9 (6.46)[e]
Postop time point + CMS	–	–	8.74 (5.26)[e]
Follow-up time point + CMS	–	–	15.6 (5.28)[c]
AIC	1841.5	1824.7	1821.8
Marginal R^2	0.224	0.290	0.295
Conditional R^2	0.607	0.650	0.692

Note:—– indicates not included in model; GA, general anesthesia; Post-op, postoperative.

[a] Values are coefficients (standard error).

[b] $P < .001$.

[c] $P < .01$.

[d] $P < .05$.

[e] $P < .1$.

The first study to evaluate the role of ASL in HCP compared 19 patients with HCP secondary to posterior fossa tumors with 16 healthy controls.[7] The former group was found to have significantly lower CBF at baseline. CBF was significantly increased in this group after "alleviation of HCP," ie, tumor resection (with additional CSF diversion in 6 patients). The present study replicates these findings, and by adding a temporal dimension in the form of multi-TI ASL, it is the first demonstration that reduction of CBF in symptomatic obstructive HCP occurs in conjunction with a prolonged arterial transit time. A regional analysis of perfusion metrics showed that CBF was lower in the HCP group for all brain regions other than the frontal and motor cortices. This finding is likely due to the raised ICP related to HCP causing reduced cerebral perfusion pressure. However, because the ICP was not directly measured in this study, we cannot provide any mechanistic evidence for this finding.

Changes in the BuxCBF in the HCP group were corresponding in direction, though only the comparison of the preoperative thalamic BuxCBF reached a level of statistical significance. BuxCBF values are inevitably higher than single-PLD CBF values because they capture blood flow in large arteries at earlier TIs. The concordance between these 2 metrics provides reassurance that the single-PLD CBF changes were not due to incomplete delivery of the labeled bolus at the PLD of 1.5 seconds.

The results of the linear multivariable mixed-effects modeling confirmed the effects of HCP on CBF seen by statistical hypothesis testing of the data. This confirmation indicated that HCP had a significant effect on CBF dependent on the time point, once age, sedation status, brain region, scanning time point, and CMS by time point were controlled for, reducing the mean CBF by 20.5 (SD, 6.27) mL/100g/min preoperatively ($P < .01$). Following tumor resection, children who had been treated with CSF diversion had significant increases in mean CBF at postoperative imaging (24.0 [SD, 5.13] mL/100g/min, $P < .001$) and at follow-up imaging (27.2 [SD, 5.18] mL/100g/min, $P < .001$).

One potential clinical implication of these results, when taken along with those of Yeom et al,[7] is that in the presence of equivocal symptomatology of raised ICP, perfusion metrics from ASL may help in decisions regarding perioperative CSF diversion. To further investigate this possibility, dedicated studies using real-time ICP measurements, ventricular volumetry, and detailed clinical correlates are needed.

Perfusion Metrics and CMS

CMS is a common postoperative complication after posterior fossa tumor resection, occurring in around one-quarter of cases.[6] The putative mechanism posits damage to the superior cerebellar peduncle at the operation as a key element causing a disturbance in cerebellocerebral circuitry. This, in turn, is thought to lead to diaschisis causing a loss of function in widespread supratentorial cortical areas, and the corollary hypoperfusion can be quantified with perfusion imaging. Thus, SPECT[11,12] and DSC-MRI[13] studies have shown frontal hypoperfusion in patients with CMS. Similarly, ASL-derived CBF was found to be reduced in the frontal lobes in a patient with CMS, recovering to normal levels after resolution of the syndrome.[15] This result was later confirmed in a small cohort study of children with posterior fossa tumors (11 patients with CMS compared with 10 without).[14] A modest reduction in CBF in the right frontal lobe was observed postoperatively, with significant increases in CBF in both frontal lobes after clinical improvement. A systematic review of 5 studies concluded that cerebral perfusion is reduced in children with CMS postoperatively, though none of the included studies incorporated preoperative comparison imaging.[29]

In this study, we were unable to replicate the findings of a statistically significant difference in postoperative CBF with respect to CMS status. However, we provide confirmatory evidence of increased CBF in children with CMS at the follow-up time point—after improvement of CMS symptoms in most—on single-PLD CBF ($P = .0403$). The multi-TI ASL results did not demonstrate any differences in BAT or BuxCBF among groups.

The presence of an unbalanced age distribution among groups may help explain the results from statistical hypothesis testing of the data. Age is known to be broadly negatively correlated with CBF in children[20] (confirmed by its significance in the final mixed-effects model with a model coefficient of −1.34), so the CMS group having a much younger mean age may have increased the CBF at all time points for this group. Other reasons for the lack of distinction in postoperative CBF include a small sample size in the CMS group, which will have hindered comparative statistical testing. Furthermore, the repeated-measures data are unbalanced due to the substantial logistic challenges in obtaining preoperative scans in many patients.

The linear mixed-effects models described above are able to circumvent this drawback to give meaningful insight into the effects of the age parameter in the cohort. The full model, which included both HCP and CMS with their time point interactions as terms, confirmed a significant increase in CBF in the CMS group at follow-up, and coefficients for the other time points almost reached the threshold for statistical significance. The results presented here indicate that future studies investigating perfusion in CMS must take clinical features such as HCP and tumor location (and therefore surgical approach) into account.

Limitations

The lack of a clear, objective determination of CMS status is a perennial issue in studies reporting neuroimaging correlates of the syndrome, and this criticism applies to this study as much as all others in the field. To mitigate this issue, the definition of CMS applied in this study was pragmatic, based on the key criterion of mutism or reduced speech output, applied contemporaneously by an experienced neurosurgical multidisciplinary team. Because the key clinical correlate in this study was a speech deficit in CMS, it is not known from the data presented here whether CBF alterations exist postoperatively in the setting of CMS symptoms other than a speech deficit. The development of a validated scoring system for CMS is essential to objectively classify CMS phenotypes and their imaging correlates.

The regional ASL analysis did not take into account laterality because the assumption was made that symmetric vasculature leads to symmetric blood delivery. This assumption is perfectly valid in healthy brains, yet it may not be entirely true in a postoperative cohort with data acquisition shortly after surgery. For instance, unilateral manipulation of major infratentorial arteries, such as the PICA, a necessary step during midline tumor approach in dissection of the posterior fossa, may have conceivably caused a degree of arterial spasm leading to a variation in CBF by laterality.

The parcellation of the brain into regions of cortical lobes in this analysis was a pragmatic one because we are ultimately interested in behavioral effects of CBF changes in this cohort. However, we recognize that the cerebral lobes are functional-not-vascular units, and interrogating perfusion on a truly vascular basis would require territorial ASL,[30] which is technically challenging, even more so in unwell perioperative pediatric patients. The multi-TI ASL acquisition was a research sequence that is not widely available, limiting the generalizability of the results.

With regard to the insights shown on CBF in symptomatic HCP in the setting of pediatric posterior fossa tumors, these findings may not be entirely generalizable to more chronic or complex HCP syndromes seen in the wider neurosurgical population, such as low-pressure hydrocephalic states,[31] or those with an altered CSF constitution, such as following subarachnoid or intraventricular hemorrhage or CNS infection. In the adult literature, there is cautionary evidence that in normal-pressure HCP, CBF measured using ASL is reduced in deep-seated brain regions[32] but that changes in CBF do not correlate with clinical improvement following shunting.[33]

Radiation therapy has been shown to affect ASL CBF in children with posterior fossa tumors,[34] and this variable, in dichotomized form due to the lack of variation in the total dose, was included in the modeling analysis. It is possible that some of the increase in CBF and BuxCBF seen at the follow-up time point will have been accounted for by this effect, though radiation therapy was a nonsignificant feature of the model and diminished model performance; therefore, it was discarded.

CONCLUSIONS

In children with posterior fossa tumors, CBF increases after tumor resection and at follow-up scanning, and it is demonstrated for the first time that this increase occurs in conjunction with a decrease in the arrival time of labeled blood to several brain regions. Given the differences in BAT in this cohort, quantification of CBF using a single-PLD method alone has serious drawbacks; here we describe a thorough approach to CBF estimation using combined multi-TI ASL. Multivariable linear mixed-effects modeling confirms that perfusion changes are more pronounced in children presenting with symptomatic obstructive HCP requiring CSF diversion. Children with CMS had significantly higher CBF at follow-up imaging, but no differences were seen in perioperative CBF compared with those without CMS. ASL shows promise as a noninvasive tool to evaluate cerebral perfusion in the setting of pediatric obstructive HCP.

Disclosure forms provided by the authors are available with the full text and PDF of this article at www.ajnr.org.

REFERENCES

1. Johnston IH, Rowan JO, Harper AM, et al. **Raised intracranial pressure and cerebral blood flow, I: cisterna magna infusion in primates.** *J Neurol Neurosurg Psychiatry* 1972;35:285–96 CrossRef Medline
2. Johnston IH, Rowan JO. **Raised intracranial pressure and cerebral blood flow, 4: intracranial pressure gradients and regional cerebral blood flow.** *J Neurol Neurosurg Psychiatry* 1974;37:585–92 CrossRef Medline
3. Grubb RL, Raichle ME, Phelps ME, et al. **Effects of increased intracranial pressure on cerebral blood volume, blood flow, and oxygen utilization in monkeys.** *J Neurosurg* 1975;43:385–98 CrossRef Medline
4. Jabre A, Symon L, Richards PG, et al. **Mean hemispheral cerebral blood flow changes after craniotomy: significance and prognostic value.** *Acta Neurochir (Wien)* 1985;78:13–20 CrossRef Medline
5. Kerscher S, Schoning M, Schuhmann M. **Raised ICP decreases cerebral blood flow volume in pediatric patients.** In: *Proceedings of the Annual Meeting of the International Society for Paediatric Neurosurgery*, Birmingham, UK. October 20–24, 2019
6. Toescu S, Samarth G, Layard Horsfall H, et al. **Fourth ventricle tumours in children: complications and influence of surgical approach.** *J Neurosurg Pediatr* 2020;27:52–61 CrossRef Medline

7. Yeom KW, Lober RM, Alexander A, et al. **Hydrocephalus decreases arterial spin-labeled cerebral perfusion.** *AJNR Am J Neuroradiol* 2014;35:1433–39 CrossRef Medline
8. Keil VC, Hartkamp NS, Connolly DJ, et al. **Added value of arterial spin labeling magnetic resonance imaging in pediatric neuroradiology: pitfalls and applications.** *Pediatr Radiol* 2019;49:245–53 CrossRef Medline
9. Robertson PL, Muraszko KM, Holmes EJ, et al; Children's Oncology Group. **Incidence and severity of postoperative cerebellar mutism syndrome in children with medulloblastoma: a prospective study by the Children's Oncology Group.** *J Neurosurg* 2006;105:444–51 CrossRef Medline
10. Gudrunardottir T, Sehested A, Juhler M, et al. **Cerebellar mutism: definitions, classification and grading of symptoms.** *Childs Nerv Syst* 2011;27:1361–63 CrossRef Medline
11. Germanò A, Baldari S, Caruso G, et al. **Reversible cerebral perfusion alterations in children with transient mutism after posterior fossa surgery.** *Childs Nerv Syst* 1998;14:114–19 CrossRef Medline
12. De Smet HJ, Baillieux H, Wackenier P, et al. **Long-term cognitive deficits following posterior fossa tumor resection: a neuropsychological and functional neuroimaging follow-up study.** *Neuropsychology* 2009;23:694–704 CrossRef Medline
13. Miller NG, Reddick WE, Kocak M, et al. **Cerebellocerebral diaschisis is the likely mechanism of postsurgical posterior fossa syndrome in pediatric patients with midline cerebellar tumors.** *AJNR Am J Neuroradiol* 2010;31:288–94 CrossRef
14. Yecies D, Shpanskaya K, Jabarkheel R, et al. **Arterial spin-labeling perfusion changes of the frontal lobes in children with posterior fossa syndrome.** *J Neurosurg Pediatr* 2019 Aug 2. [Epub ahead of pirnt] CrossRef Medline
15. Watanabe Y, Yamasaki F, Nakamura K, et al. **Evaluation of cerebellar mutism by arterial spin-labeling perfusion magnetic resonance imaging in a patient with atypical teratoid/rhabdoid tumor (AT/RT): a case report.** *Childs Nerv Syst* 2012;28:1257–60 CrossRef Medline
16. Alsop DC, Detre JA, Golay X, et al. **Recommended implementation of arterial spin-labeled perfusion MRI for clinical applications: a consensus of the ISMRM perfusion study group and the European consortium for ASL in dementia.** *Magn Reson Med* 2015;73:102–16 CrossRef Medline
17. Dale AM, Fischl B, Sereno MI. **Cortical surface-based analysis.** *Neuroimage* 1999;9:179–94 CrossRef Medline
18. Modat M, Cash DM, Daga P, et al. **Global image registration using a symmetric block-matching approach.** *J Med Imaging (Bellingham)* 2014;1:024003 CrossRef Medline
19. Buxton RB, Frank LR, Wong EC, et al. **A general kinetic model for quantitative perfusion imaging with arterial spin-labeling.** *Magn Reson Med* 1998;40:383–96 CrossRef Medline
20. Hales PW, Kawadler JM, Aylett SE, et al. **Arterial spin-labeling characterization of cerebral perfusion during normal maturation from late childhood into adulthood: normal "reference range" values and their use in clinical studies.** *J Cereb Blood Flow Metab* 2014;34:776–84 CrossRef Medline
21. Jenkinson M, Bannister P, Brady M, et al. **Improved optimization for the robust and accurate linear registration and motion correction of brain images.** *Neuroimage* 2002;17:825–41 CrossRef Medline
22. R Core Team. **A language and environment for statistical computing.** R Foundation for Statistical Computing; 2017. https://www.r-project.org/. Accessed March 3, 2020
23. Barton K. **MuMIn: Multi-Model Inference.** 2020. https://cran.microsoft.com/snapshot/2020-11-30/web/packages/MuMIn/index.html. Accessed March 3, 2020
24. Rao VK, Haridas A, Nguyen TT, et al. **Symptomatic cerebral vasospasm following resection of a medulloblastoma in a child.** *Neurocrit Care* 2013;18:84–88 CrossRef Medline
25. Gocmen S, Acka G, Karaman K, et al. **Cerebral vasospasm after posterior fossa tumor surgery: a case report and literature review.** *Pediatr Neurosurg* 2020;55:393–96 CrossRef Medline
26. Deghedy M, Pizer B, Kumar R, et al. **Basilar artery vasospasm as a cause of post-operative cerebellar mutism syndrome.** *Case Rep Pediatr* 2022;2022:9148100–05 CrossRef Medline
27. Lin CT, Riva-Cambrin JK. **Management of posterior fossa tumors and hydrocephalus in children: a review.** *Childs Nerv Syst* 2015;31:1781–89 CrossRef Medline
28. Borgesen SE, Gjerris F. **Relationships between intracranial pressure, ventricular size, and resistance to CSF outflow.** *J Neurosurg* 1987;67:535–39 CrossRef Medline
29. Ahmadian N, van Baarsen M, Robe, PA, et al. **Association between cerebral perfusion and paediatric postoperative cerebellar mutism syndrome after posterior fossa surgery: a systematic review.** *Childs Nerv Syst* 2021;37:2742–51 CrossRef Medline
30. Hartkamp NS, Petersen ET, De Vis JB, et al. **Mapping of cerebral perfusion territories using territorial arterial spin-labeling: techniques and clinical application.** *NMR Biomed* 2013;26:901–12 CrossRef Medline
31. Pang D, Altschuler E. **Low-pressure hydrocephalic state and viscoelastic alterations in the brain.** *Neurosurgery* 1994;35:643–56 CrossRef Medline
32. Virhammar XJ, Laurell XK, Ahlgren XA, et al. **Arterial spin-labeling perfusion MR imaging demonstrates regional CBF decrease in idiopathic normal pressure hydrocephalus.** *AJNR Am J Neuroradiol* 2017;38:2081–88 CrossRef Medline
33. Virhammar J, Ahlgren A, Cesarini KG, et al. **Cerebral perfusion does not increase after shunt surgery for normal pressure hydrocephalus.** *J Neuroimaging* 2020;30:303–07 CrossRef Medline
34. Li MD, Forkert ND, Kundu P, et al. **Brain perfusion and diffusion abnormalities in children treated for posterior fossa brain tumors.** *J Pediatr* 2017;185:173–80.e3 CrossRef Medline